Estimating land surface energy fluxes in SE Spain using Aster and MODIS data

Mónica García [a] , Sergio Contreras [a], Francisco Domingo [a] and Juan Puigdefábregas [a]

[a] Estación Experimental de Zonas Áridas. CSIC. General Segura 1. Almería 04001. Spain.
monica@eeza.csic.es

ABSTRACT

Land degradation can be associated with decreases in water use efficiency by ecosystems, with impacts on actual evapotranspiration or latent heat. As this should be reflected in the partition of surface energy fluxes, indicators of land degradation based on energy ratios could help to monitor land condition. In this study, we test a simple operational model for calculating energy fluxes in a semiarid region, in mountainous terrain, at two different spatial resolutions (90 m and 1 km), using Aster and MODIS data on 18-07-2004.

Results show that Aster and MODIS results are comparable within reported instrumental errors. However, the lost of detail is remarkable. If the processes of land degradation related with changes in the surface energy balance are explicit at 1 km, which needs further elucidation, MODIS is an adequate tool to perform regional assessments by means of its high temporal and spatial coverage. Comparisons with field data show low net radiation errors (within pyranometer precision) and large errors for sensible heat (using eddy covariance technique) but within the ranges obtained by other authors.

The spatial patterns for the ratio H/Rn (sensible heat to net radiation) proposed as an indicator of land condition are coherent with the surface type. Potentially degraded sites are in the radiation controlled domain at this time of the year, which provides some insight about their energy partition. Preliminary comparisons at 1 km of the rescaled H/Rn index by aridity levels with an independent indicator of land degradation based on Rainfall Use Efficiency (RUE) show promising results. Because, of the limited verification data and dates, the model results are preliminary and need further testing.

Keywords: sensible heat, net radiation, surface fluxes, Aster, MODIS, semi-arid.

1 INTRODUCTION

Currently, there is a lack of standard and operational procedures for monitoring land degradation over large regions [1]. Land degradation processes are the consequence of permanent alterations in the optimum structure and functioning of ecosystems leading to decreases in its resource use efficiency and productive capacity. Some of these changes, mostly human driven, can be related to ecosystem functional indicators based on the hydrologic cycle [2,3] or the surface energy balance. Both types of indicators are connected through the latent heat flux (LE) or evapotranspiration. Calculation of surface energy ratios requires spatially disaggregated estimates of surface energy balance components on monthly and annual scales compatible with the temporal scales of desertification.

The law of conservation of energy states that the available energy reaching a surface is dissipated mainly as latent heat (LE) and sensible heat (H): Rn-G = LE+H . Being, Rn net radiation, G soil heat flux and Rn-G available energy. The algorithms to calculate these energy components use information in the solar and thermal range, being remote sensing the only data source providing radiometric temperature and vegetation cover observations over large extents. This is crucial as explains most of the partition of the available energy into sensible and latent heat [4].

The most vulnerable areas to land degradation are located in arid regions (UNCCD) where the development of an operative system would require data such as MODIS (Moderate Resolution Imaging Spectrometer), available at high temporal resolution but with 1 km pixel size. This questions the validity of models originally designed for agricultural areas or almost ideal conditions when these models are applied over arid regions and heterogeneous sites with sparse vegetation covers [5].

In this study, we test a simple operational model [6,7,8] for calculating energy fluxes in a semi-arid region at two different spatial resolutions (90 m and 1 km). To select an appropriate energy balance indicator, it is important to note the low value of latent heat fluxes during several months in semi-arid areas. For instance in the study region latent heat is within error level of models during several days [9].

For this reason, we explore the H/Rn ratio as an indicator for land degradation. Most authors assume that daily soil heat fluxes (G) are zero [4]. Therefore, the evaporative fraction (EF), defined as the ratio of latent heat (LE) and available energy (Rn-G), can be expressed as EF=LE/Rn; being the H/Rn =1-EF. The reason for not using EF=1-H/Rn as an indicator is twofold: in semiarid areas the contribution of G cannot be neglected [10]; and latent heat is usually within model errors as was pointed out before. We preferred to use the index H/Rn, that should present a wider range of variability than EF and a higher signal-to-noise ratio without making any assumption about G,.

We hypothesize that the increase in bare soil due to decreases in vegetation cover taking place as a consequence of land degradation should increase surface temperature and albedo causing increases in H, and decreases in Rn similarly to results presented by [11] in the Sahel. Feedback effects, such as those occuring between albedo and surface temperature might counterbalance some of these impacts. This work pretends to elucidate some of these aspects. The specific objectives are:

(1) Evaluate the performance of a simple energy balance algorithm in a semi-arid region in SE Spain characterized by its land cover heterogeneity, fragmentation and mountainous terrain on a daily basis.

(2) Compare results derived from finer to coarser resolution data. In particular, 1 km MODIS versus 90 m Aster (Advanced Spaceborne Thermal Emission and Reflection Radiometer) to estimate land surface energy fluxes.

Aster is currently, the only sensor collecting multispectral thermal infrared data at high spatial resolution being very appropriate for testing of models and direct ground comparisons [12]. On the other hand, Aster and MODIS are on board the Terra platform, allowing analyses of scale. Recent work has been done to compare boths sensors showing good agreement (<1 K) [13]. It is desirable to extend this type of comparisons to other variables and regions.

2 STUDY SITE AND DATA

The study region (Figure 1) located in South East Iberian Peninsula (Almería, Spain) comprises 3600 km^2 (36.95º N, 2.58ºW). This region is characterized by its heterogeneity, due to the abrupt relief changes with altitudinal gradients ranging from sea level up to 2800 m (a.s.l.) in Sierra Nevada mountain. The precipitation and temperature regimes present wide contrasts driven by the orography [14]. Annual precipitation is the lowest in the Tabernas desert, with less than 200 mm, while in the mountains can be enough to sustain forest growth, ranging between 400 mm up to 700 mm.

In the center of the study site, the Gador mountain range covers 552 km^2, composed of shrubland and perennial grassland vegetation, some oak relicts, reforested areas of pine woods, and some semi-abandoned orchards. The study site includes part of the Natural Park of Sierra Nevada including wood of pines, oak relicts, and shrublands. In the northeast is the Tabernas desert with a complex topography comprising an area of badlands. Along the Andarax ephemeral river which flows by Almeria city, there is a mosaic of citrus orchards and vinegrapes. One of the most outstanding features of the scene is the large plastic greenhouse area covering more than 330 km^2. This unique combination allows using this area as a pilot site where to test a simple model for calculating surface energy fluxes that could be extended for use at regional and global scales.

For this study, we have used Aster and MODIS data acquired on July-18th-2004 at 11.00 UTC. The Aster products used were 2AST07 which is Surface reflectance at 15 m (VNIR) and 30 m (SWIR), and 2AST08 Kinetic temperature at 90 m. Two MODIS products were used: the 8 day surface reflectance at 500 m (MOD09) instead of daily, to decrease errors as albedo and vegetation indices can be assumed constant during this time. The other product used was daily land surface temperature product (MOD11). In the case of MODIS, surface temperature errors range from 1 -3 K with no incidences for ASTER, where the reported absolute precision is 1-4 K.

A digital elevation model (DEM) from USGS (United States Geological Survey) available at 30 m resolution and a digital orthophoto (from the Andalusian Regional Government) at 0.5 m were used at different stages of the study.

Instrumental field data are acquired continuously at the Gador Experimental site since 2003 (Figure 1, upper right panel). They were used to compare with model results. The eddy covariance technique was used to measure latent and sensible heat flux using a three dimensional sonic anemometer CSTAT3 and a krypton hygrometer KH20, both from Campbell Scientific Inc., USA. The tower is located in a flat area covered with perennial grasslands and shrubs so that the measurements acquired at that point include an area of 2 km^2, existing several areas with similar vegetation type within the Gador mountain. Net radiation (NR-LITE; Kipp & Zonen, Delft, the Netherlandstemperature), and relative humidity (thermohygrometer HMP 35C, Campbell Scientific, Logan, UT, USA) sonic and soil temperature (SBIB sensors) are also continuously measured at the site. Besides air temperature measurements at the Gádor Mountain range field site, air temperature was measured from other 10 meteorological stations at the time of the satellite overpass (11.00 UTC).

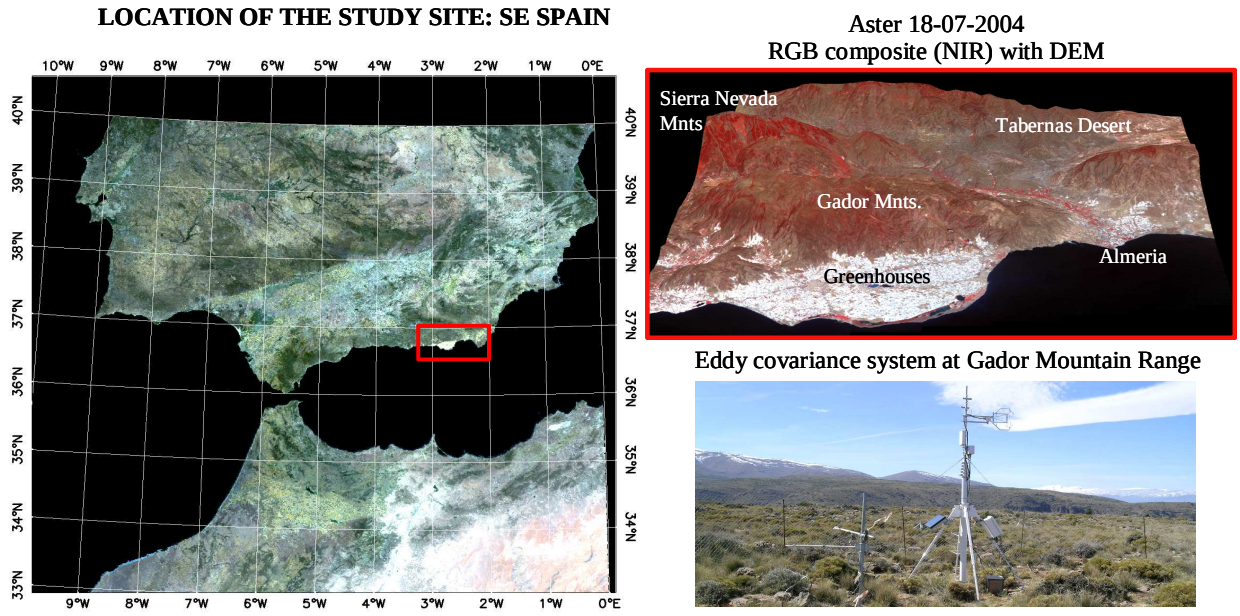

Figure 1: Location of the study site in South East Spain, Almeria province. The upper right panel shows MODIS True Color Composite corresponding to the study site and 18-07-2004. The lower right panel shows the location of the eddy covariance system for sensible and latent heat in a flat area at the Gador Mountain range.

3 METHODS

First, Rn, H and its ratio H/Rn were calculated for Aster and MODIS. In a second step, the results obtained with Aster were linearly aggregated into a 1 km pixel to compare with MODIS. Finally, results of H/Rn at 1 km were rescaled according to aridity levels to compare with an independent land degradation indicator.

3.1. Estimation of Net Radiation

Rn is calculated as the balance between incoming (↓) and outgoing fluxes (↑) of shortwave (Rs) and longwave (Lw) radiation. By agreement, incoming fluxes are positive and outgoing negative. This can be expressed as the sum of Shortwave (Rns) and Longwave net radiation (Lnw)

$$Rn = Rs\uparrow + Rs\downarrow + Lw\downarrow + Lw\uparrow = Rns + Lnw \quad (1)$$

Shortwave Net radiation

The shortwave net radiation using remote sensing is calculated as: $Rns=(1-\alpha)\, Rs\downarrow$. Where α is the broadband surface albedo, estimated according to [15] for 6 Aster and MODIS bands. $Rs\downarrow$ (incoming solar radiation) was estimated using a solar radiation model from [16].

Longwave Net radiation

The longwave energy components are related to surface and atmospheric temperatures through the Stephan-Boltzmann law. The longwave net radiation is calculated as in (2):

$$Lnw = -\varepsilon_s \sigma T_s^4 + Lw\downarrow \quad (2)$$

Where broadband emissivity for the surface (ε_s) was estimated based on a logarithmic relationship with NDVI [17] and radiometric surface temperature (Ts) was directly obtained from Aster and MODIS LST (Land Surface Temperature) products calculated with the TES (Temperature Emissivity Separation) algorithm for Aster and the day/night LST algorithm for MODIS. An empirical function is used for the incoming longwave radiation Lw [18].

Air temperature

To avoid relying on meteorological information, air temperature was estimated from the images using the triangle NDVI-Ts proposed by [8]. The apex of the NDVI-ts space (high NDVI and low temperature) should correspond to pixels with high NDVI located at the wet edge of the triangle, and can be assumed to be at the air temperature [19]. Due to the altitudinal gradients it is necessary to apply a correction to air temperature considering as a base or

reference altitude that of the pixels at the apex. Afterwards, positive corrections for altitude are made for pixels below the base altitude and vice-versa for pixels above using the rule of thumb of 6.5 ºC each 1000 m. This is better than approaches considering a unique air temperature for the whole area assuming constant meteorological conditions at the blending height [8, 20] and also works better than [21] dry and wet pixel approach, probably more suited for flat areas, evaluated in preliminary tests (results not shown).

3.2. Estimation of Sensible Heat flux

H can be estimated by a model of turbulent transport from the surface to the lower atmosphere based on surface layer similarity of mean profiles of temperature and wind speed using a resistance form:

$$H = \cdot\rho\cdot c_p \cdot \frac{(Ts-Tair)}{r_h} \quad (3)$$

Where Ts is land surface temperature, Tair is air temperature, both at the time of image acquisition, r_h is the atmospheric resistance to the transfer of H, ρ and c_p are air density and specific heat at constant pressure respectively. B can be defined as an exchange coefficient to sensible heat transfer [6, 7]: $B=\cdot\rho\cdot c_p\cdot h_a$

Being h_a the turbulent exchange coefficient dependent on wind velocity, aerodynamic roughness length, roughness length for heat transfer and Monin-Obukov length. As having estimates of these variables at large scales is impossible, more operational parameterizations have been proposed. We used the [8] approach which states that the main factor affecting conductance to heat transfer is vegetation cover and establishes a linear relation between the exchange coefficient to sensible heat transfer B and fractional cover.

3.3. Relation of H/Rn at 1 km with land degradation

To provide some preliminary insights of the relation of the H/Rn ratio with potentially degraded areas at 1 km, we compared in the study site the H/Rn ratio at 1 km with a land degradation index based on the concept of RUE (Rainfall Use Efficiency) expressed as NDVI / Precipitation [22].
First, it was necessary to rescale the H/Rn ratio according to the aridity index to make comparisons across different regions (e.g. forest, desert). The aridity index was calculated as the ratio between potential evapotranspiration [23] and average annual precipitation interpolated from the stations at the site.
The assumption below rescaling H/Rn by aridity index levels is that in the scene there is enough variability as to find degraded and non-degraded sites. Therefore, within each aridity index level there is range of variation from optimum levels (low H/Rn) to degraded (high H/Rn). Quantile regression for the 5 % and 95 % were performed to find the enveloping functions.

The rescaled H/Rn is: $$H / Rn_{resc} = \frac{H / Rn_{obs} - H / Rn_{5\%}}{H / Rn_{95\%} - H / Rn_{5\%}} \quad (4)$$

Where: H / Rn_{obs} is the observed value of H/Rn in the pixel.

$H / Rn_{5\%}$ is the value of H/Rn lower enveloping function for the aridity level corresponding to that pixel.

$H / Rn_{95\%}$ is the value of H/Rn upper enveloping function for the aridity level corresponding to that pixel.

The land degradation index has two dimensions: RUE_{mean} or the average RUE for a four year period, related with annual productivity or biomass, and RUE_{max} or the maximum monthly RUE within that four year period that could be related with maximum productivity. Sites with low RUE_{mean} or low RUE_{max} could be potentially degraded sites. [22] estimated maximum productivity and annual biomass using NDVI on a 1 km pixel level from AVHRR. For comparison with H/Rn the RUE was used in a qualitative way, with low, mean and high classes of both indices: RUE_{mean} and $RUE_{max.}$

4 RESULTS

4.1. Comparison of air temperature with field data

Eleven meteorological stations were used to evaluate air temperature (Tair) estimations at the time of the Terra satellite overpass (11.00 UTC). First, the temperature of the apex according to [8] was selected (Figure 2). Afterwards, corrections for altitude improved the overall error from to less than 2 ºC (Table 1).

The overall adjustment is good, but Tair estimates are subjected to local errors. One concern is that altitude is not the only factor affecting Tair. Nevertheless, using this approach presents the advantage of relief from using ancillary data. Also any systematic error in Ts estimation will propagate in the Tair; therefore, these errors should cancel out when calculating differences Ts-Tair for estimating sensible heat flux.

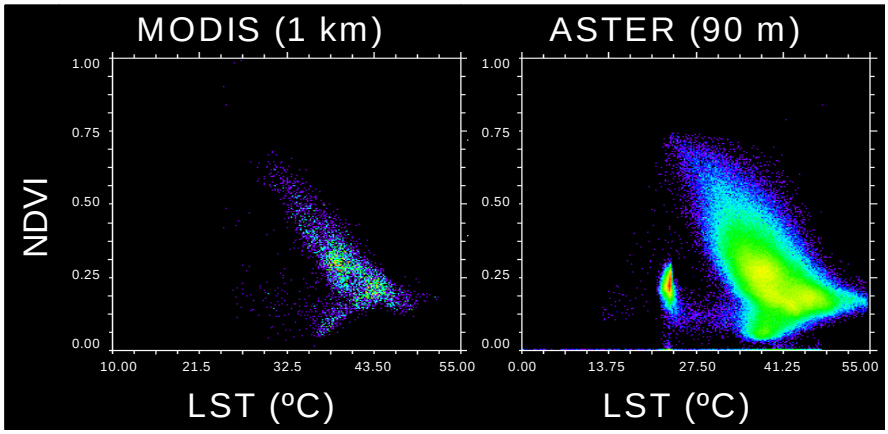

Figure 2: MODIS and ASTER NDVI-LST (Land Surface Temperature) triangle to extract apex temperature values (minimum temperature with higher NDVI) according to [8].

Table 1: Air temperature estimates. "T bias before adjustment" is the absolut average difference of the residuals between estimated air temperature and measured air temperature. "T bias after adjustment" is the absolut average difference of the residuals between estimated air temperature after applying a correction factor by altitude.

	ASTER	MODIS
R^2 ($T_{\text{air stations}}$ and altitude)	0.61	
T bias before adjustment (ºC)	4.31	2.45
T bias after adjustment (ºC)	1.96	1.91
T apex (ºC)	24	28.5
Base altitude (m)	1800	800

4.2. Model performance with MODIS and Aster at the Gador Mountain range field site

At the Gádor Mountain range field site (see Figure 1, lower right panel), Rn and surface energy fluxes were measured and compared with Aster and MODIS estimates (Table 2). The B values obtained at the Gador Mountain range field site are reasonable as they are similar to the fixed value of 0.25 proposed by [7] for dryland and irrigated crops in France and much lower than the fixed value of 0.64 of [6] in irrigated wheat fields in Arizona.

Table 2: Comparisons between measured and estimated values at the Gádor Mountain range field site. B is the exchange coefficient for heat transfer, Rn is net radiation and H is sensible heat flux.

	Sensor	B	Rn (W m-2)	H (W m-2)
Values	Aster	0.250	189.86	107.65
	MODIS	0.2407	172.73	84.42
	Measured	0.370*	179.72	152.97
Error (differences)	Aster-Measured	-0.06	10.14	-45.33
	Modis-Measured	-0.069	-6.99	-68.56
	Modis-Aster	0.0093	-17.13	-23.23
Error (%)	Aster-Measured	-24.00	5.34	-42.11
	Modis-Measured	-18.65	-3.89	-44.82
	Modis-Aster	3.72	-9.02	-21.58

**Estimated empirically from field data at Gádor Mountain range field site*

In the Gador mountain range field site, errors are very low for Rn (around 5% compared to field data) and therefore within reported pyranometer errors (±10 % and directional error of < 25 W m^{-2}). In this site, both Aster and MODIS underestimate H when comparing with eddy covariance measurements. Although errors for Ts are within acceptable quality levels reported for Aster and MODIS, otherwise pixels were masked, it would be necessary to evaluate its influence in H and Rn estimates in future studies. We also have to be aware that the eddy covariance technique is subjected to uncertainty levels of 20-30 % [24]. Moreover, in semi-arid areas with sparse vegetation cover, error in energy fluxes tend to be on the higher side of this range around 30 % [25].

In general, the range of errors reported by other authors in H flux is very variable. [26] consider around 50 Wm^{-2} an acceptable error for H. In the literature, errors in the best cases are around 22 Wm^{-2} [4] and can reach up to 50% even with sophisticated models if parameterizations are not good. Using a fixed value for kB^{-1} in agricultural areas produces errors as high as 150 Wm^{-2} or 43-64 Wm^{-2} [26]. [27] obtained a RMSE of 43.35 W m^{-2} for sensible heat. [28] in the Great Basin desert got errors in H around 40 % similarly to our results.

4.3. Analysis of the H/Rn spatial patterns

The assessment of model results cannot be made solely on the basis of a unique, although very representative of the study site, eddy covariance value. To evaluate the spatial coherence of the results obtained with Aster, comparison of values for different land use types has been performed (Figure 3). These sites were selected by photo-interpretation based on field knowledge of the area.

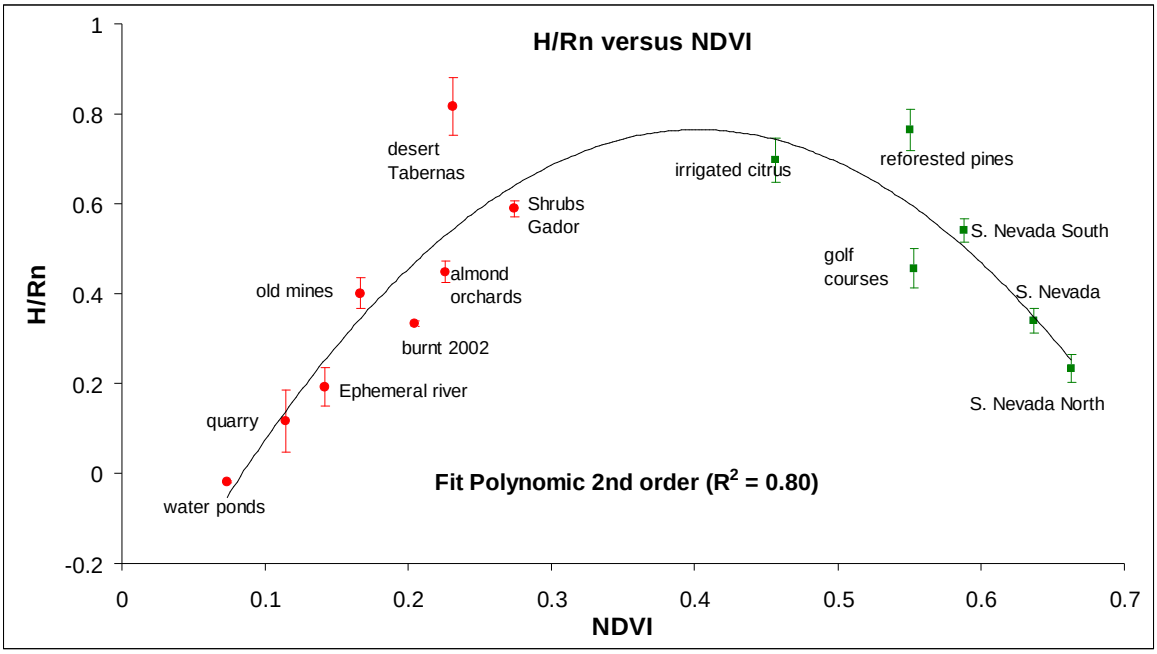

Figure 3: H/Rn versus NDVI for different vegetation types. The surface type legend is close to each value. Error bars represent the confidence interval ($p< 0.05$). 2nd order polynomial fitting for mean values presents an $R^2 = 0.80$. Red dots represent the part of the curve controlled by radiation and green squares by evapotranspiration. There is a threshold for NDVI (0.4). Before the threshold the H/Rn increases with vegetation cover, after it the ratio H/Rn decreases.

In general, H/Rn patterns are consistent and resemble the pattern of a radiation and an evaporation controlled branch related with direct and feedback effects between albedo and surface temperature [20, 21]. At the study site, the highest evaporative surface are the water ponds that can be considered a calibration site with zero values of H/Rn (Figure 3). Then, there is a trend to increase the partition of H to Rn with increasing vegetation cover. These surfaces present high albedo values, e.g. the cement quarry, and in this date the soil is dry, and the increase in vegetation cover tends to increase surface roughness, and in consequence the driving force for H flux [8]. However, this sparse vegetation is not evaporative, being reasonable to expect increases in G. This trend occurs up to a threshold in which either vegetation cover is evaporative (trees with deep roots or the irrigated crops). Then, the H/Rn tends to decrease with increasing vegetation cover responding to a situation in which the surfaces are evaporating water.

It is remarkable the influence of aspect on the surface energy fluxes. Thus, in the Sierra Nevada mountain, those pixels located in northern aspects show lower H/Rn ratio than those at southern or Mediterranean face. The golf courses present H/Rn values similar to almond crops but their LAI is low enough to have a strong soil influence. It is surprising that the irrigated citrus orchards located by the Andarax ephemeral river present higher values than for instance dryland almonds. The reason is the high degree of land fragmentation (parcels are in general smaller than 1 ha) alternating bare soil and citrus orchards.

Figure 3 shows that the H/Rn index captures spatial patterns related with surface energy partition. However, solely this index is not good to discriminate among cover types, and a combination with a vegetation cover index

helps to evaluate if the surfaces are in the evaporative or in the radiation controlled domain. On the other hand, the plot albedo-Ts did not show the expected bell-shaped pattern (results not shown) which appears very clearly in the H/Rn –NDVI plot. Potentially degraded sites such as abandoned mines, the cement quarry, or the burnt scar from the 2002 fire (Figure 3) are all in the radiation controlled branch at this time of the year. This provides some insight about their radiation balance.

4.4. Comparison between MODIS and ASTER performance

Comparisons between Aster and MODIS were performed by resampling the Aster pixel size of 90 m using a cubic convolution filter into MODIS 1 km pixel size.

Results in Table 3 show that for the set of input variables MODIS values tend to be slightly higher than Aster. It is remarkable the RMSE in Ts of almost 2.90 ºC. These differences are translated in the output variables causing underestimations of MODIS with respect to Aster. Most of the input variables present a good R^2, which means that the input variables aggregate linearly at least to explain between 0.63-0.70 of the variance. However, there is a remaining ~30 % of the variance responding to non-linear aggregation effects combined with sensor differences in sensor performance and correction algorithms employed. These differences in input values between MODIS and Aster are amplified in the output values of surface energy fluxes of H, Rn and H/Rn (Table 3).

In any case, both RMSE and mean differences are within reported pyranometer precision for Rn. RMSE results for H are comparable to some closure errors in energy balance using eddy covariance technique [23]. This means that despite some differences between Aster and MODIS sensor performance, combined with the impact of change in spatial resolution, the two sensors provide similar results, for spatial features of 1 km or larger, comparable to repeatability of instrumental data.

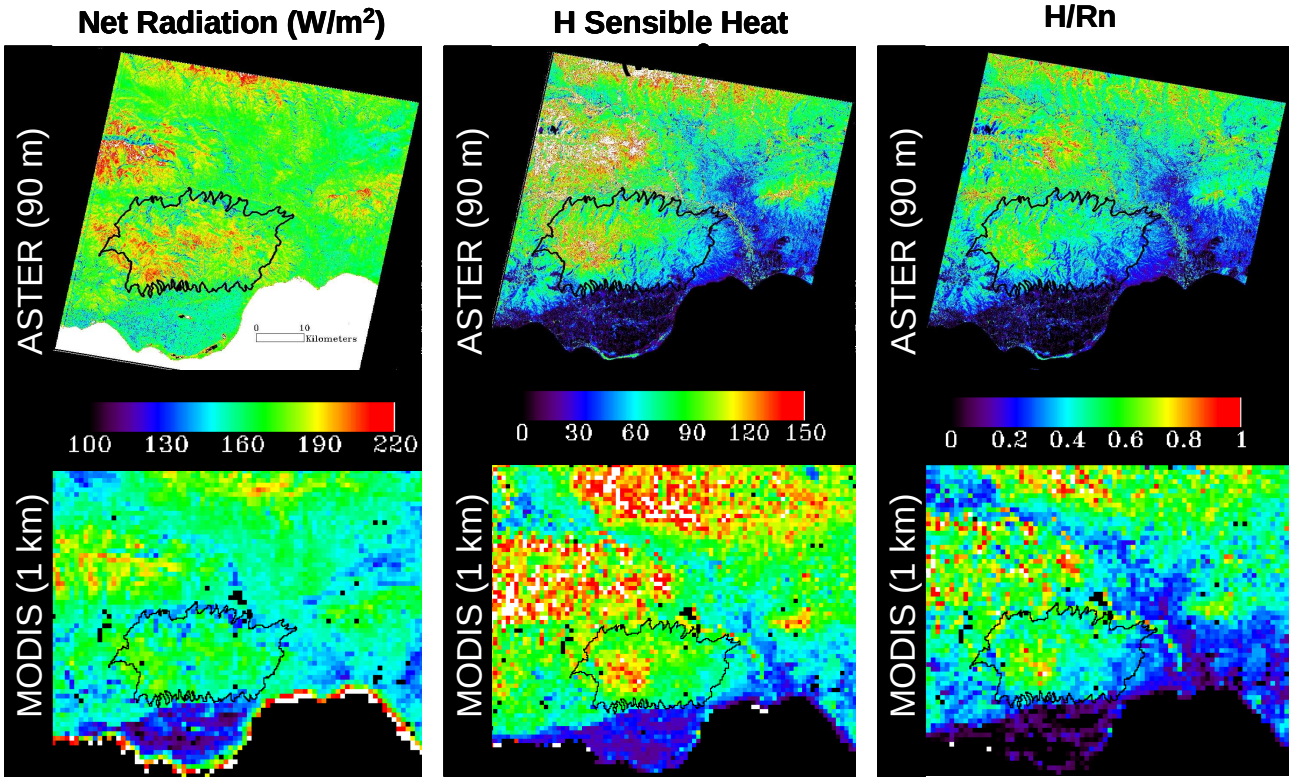

Figure 4: Comparison of spatial patterns of net radiation, sensible heat and H/Rn ratio for ASTER (90 m) and MODIS (1 km) over the study site on 18-07-2004. The Gador mountain range is outlined with a black line.

Figure 4 shows results for output variables using Aster and MODIS. The gross main structure of the surface fluxes explained by the H/Rn partition is maintained from MODIS to Aster scene, but level of detail is not comparable. For this reason, features with a spatial resolution lower than 1 km are not resolved (e.g the mosaic of irrigated citrus and bare soil by the Andarax river). Therefore, if the processes of land degradation related with changes in the surface energy balance are explicit at 1 km grains, which needs further elucidation, MODIS can be consider an adequate tool to perform regional assessments by means of its high temporal and spatial coverage.

Table 3. Input and output variables for MODIS and Aster: LST (Land Surface Temperature), B (exchange coefficient to sensible heat transfer), H (sensible heat flux), Rn (net radiation), RMSE (Root Mean Square Error). Diff. Mean value is the average of differences between MODIS and ASTER, R^2 the Pearson coefficient after aggregation of Aster to 1 km pixel.

VARIABLES		Diff. Mean Value	RMSE	R^2
INPUT	**LST (ºC)**	0.277	2.90	0.65
	Broadband Albedo	0.0214	0.0020	0.63
	B (mm/ºC)	-0.009	0.0028	0.74
	Emissivity	0.0047	0.0117	0.70
OUPUT	**H (W m-2)**	-10.08	27.019	0.58
	Rn (W m-2)	-13.37	18.59	0.34
	H/Rn	-0.017	0.025	0.39

4.5. Relation of H/Rn at 1 km with land degradation

The H/Rn was rescaled by aridity levels to compare across land cover types, using enveloping functions (Figure 5) polynomic for the lower (5% quantile) and linear for the upper level (95% quantile).

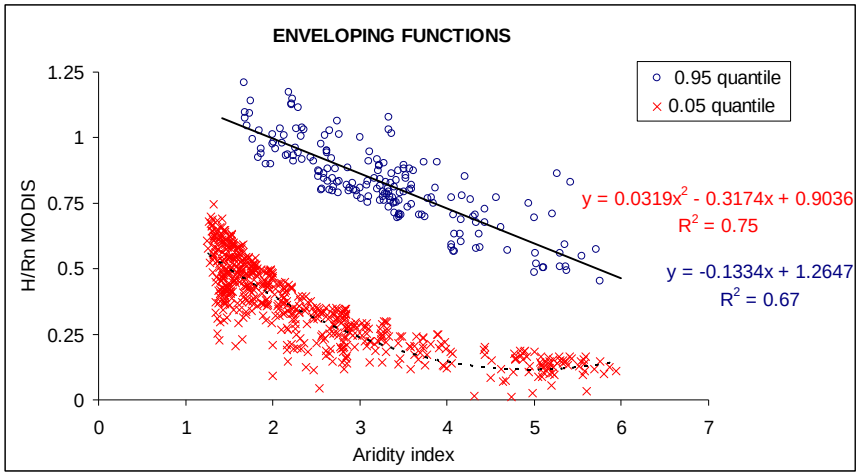

Figure 5: Enveloping functions used to rescale the H/Rn index by aridity levels. They were calculated using quantile regression to find the upper and lower boundaries. For the upper boundary (95 % quantile) a 2nd degree polynomic function was fitted. For the 5 % quantile (lower boundary) a linear regression was fitted.

The H/Rn rescaled presents high values for low RUE_{mean} values and vice-versa. For the mean class of RUE_{mean}, H/Rn is also high (Figure 6). The relations of H/Rn with RUE_{max}, are only apparent when annual productivity (RUE_{mean}) is low or mean showing a decreasing trend along increasing RUE_{max}. This index seems promising in capturing some of the alterations of the energy balance related with potentially degraded sites, being mostly in agreement with the hypothesis regarding the behavior of H/Rn in degraded areas.

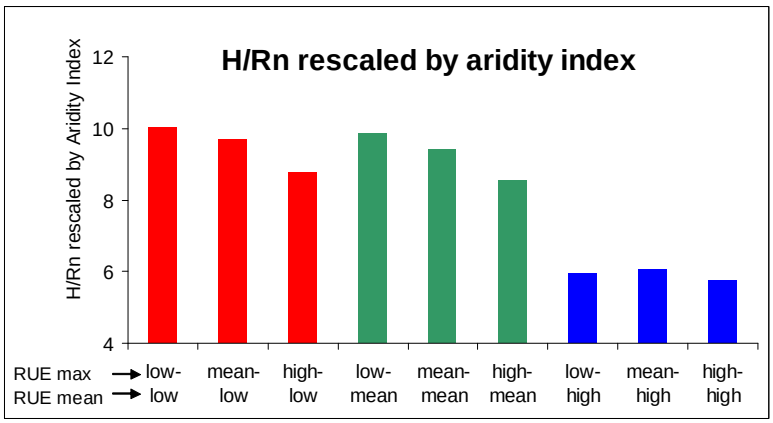

Figure 6: Comparison of the H/Rn ratio rescaled by the aridity index enveloping functions with classes of the RUEmean (Mean Rainfall Use Efficiency) and RUEmax (Maximum Rainfall Use Efficiency) at 1 km over the study site.

5 CONCLUSIONS

Comparison between MODIS and Aster spatial patterns of surface energy balance components on 18-07-2004 reveals that the main structure is maintained from Aster to MODIS. However, the lost of detail is remarkable and features smaller than 1 km are not resolved. Regarding RMSE values between Aster and MODIS, net radiation values are within reported pyranometer precision and sensible heat flux are comparable to closure errors in energy balance using eddy covariance technique [24]. Therefore, if the processes of land degradation related with changes in the surface energy balance are explicit at grains of 1 km, MODIS is an adequate tool to perform regional assessments by means of its high temporal and spatial coverage.

Comparison with field data using eddy covariance technique at the Gador experimental field site shows very low net radiation errors (within pyranometer precision). Sensible heat provides larger errors but within the ranges obtained by other authors [13¸28], being Aster within the threshold of 50 Wm^{-2} proposed by [26]. To decrease errors in sensible heat flux, it will be desirable to improve estimations of the exchange coefficient to sensible heat flux. Air temperature can be extracted from the images using the NDVI-Ts space relationship [8] corrected by altitude with an acceptable overall error (< 2 ºC).

The spatial patterns of Aster H/Rn (sensible heat/net radiation) index are coherent with the type of surface. However, solely this index is not good to discriminate among these cover types, and a combination with a vegetation index helps to evaluate whether surfaces are in the evaporative or in the radiation domain [21].

Potentially degraded sites are in the radiation controlled domain (positive H/Rn-NDVI slope) at this date, which provides some insight about their energy partitioning. In addition, preliminary comparisons at 1 km of the rescaled H/Rn index by aridity levels with an independent indicator of land degradation based on rainfall use efficiency show promising results. However, because of the limited verification data currently available, the model results are preliminary and in need of further testing.

Establishing a robust land degradation index needs additional analysis including several dates to fully understand the interaction between water and energy at different surfaces. Efforts should be devoted to scale daily results to temporal scales compatible to the time scale of land degradation processes. Along this line, a remaining question is the spatial and temporal scales in which alterations of energy balance fluxes related with land degradation are explicit.

Acknowledgments

This research is within the EU project DeSurvey (A Surveillance System for Assessing and Monitoring of Desertification; FP6-00.950). The authors wish to thank Dr. del Barrio, M. San Juan and Dr. Lazaro for their help.

REFERENCES

[1] PUIGDEFÁBREGAS, J., MENDIZÁBAL, T. 2004: Prospects for desertification impacts in Southern Europe. In A.Marquina (ed): *Environmental challenges in the Mediterranean 2000-2050*, chapter 10, pp 155-172, Kluwer Academic Publisher, Netherlands.

[2] SHARMA, K. D., 1998: The hydrological indicators of desertification. *J. Arid Environ. 39*, pp.121-132.

[3] BOER, M.M. AND PUIGDEFABREGAS, J., 2003: Predicting potential vegetation index values as a reference for the assessment and monitoring of dryland condition. *Int. J. Remote Sens. 24* (5), pp. 1135 – 1141

[4] KUSTAS W.P. Y J.M. NORMAN. 1996: Use of remote sensing for evapotranspiration monitoring over land surfaces. *Hydrolog Sci J*. 41(4), pp. 495-516.

[5] CHEHBOUNI, A.; LOSEEN, D.; NJOKU, E.G.; LHOMME, J.P.; MONTENY, B.; AND KERR,Y.H., 1997: Estimation of sensible heat flux over sparsely vegetated surfaces. *J. Hydrol. 89*(1-4), pp. 855-868.

[6] JACKSON, RD; REGINATO, RJ; IDSO, SB., 1977: Wheat Canopy Temperature: A Practical Tool for Evaluating Water Requirements. *Water Resour. Res. 13 (3)*, pp. 651-656,

[7] SEGUIN, B. AND ITIER, B., 1983: Using midday surface temperature to estimate daily evaporation from satellite thermal IR data. *Int. J. Remote Sens. 4*, pp. 37-383.

[8] CARLSON, T.N., CAPEHART, W.J., AND GILLIES, R.R., 1995: A New Look at the Simplified Method for Remote-Sensing of Daily Evapotranspiration. *Remote Sens. Environ. 54*, pp. 161-167.

[9] DOMINGO, F., VILLAGARCÍA, L., BOER, M., ALADOS-ARBOLEDAS, L., PUIGDEFÁBREGAS, J. 2001: Evaluating the long-term water balance of arid zone stream bed vegetation using evapotranspiration modelling and hillslope runoff measurements. *J. Hydrol. 243*, pp. 17 - 30.

[10] WAASSENAAR, T., OLIOSO, A., HASAGER, C., JACOB, F., CHEHBOUNI, A. 2002: Estimation of evapotranspiration on heterogeneous pixels. *Proceedings of the 1st Symposium of Recent advances in Quantitative Remote Sensing. Valencia*, Sept 2002. Sobrino, Ed, pp. 319-328.
[11] DOLMAN A.J., GASH J.H.C., GOUTORBE, J.P., KERR Y, LEBEL T, PRINCE SD, AND STRICKER, J.N.M., 1997: The role of the land surface in Sahelian climate: HAPEX-Sahel results and future research needs. *J. Hydrol. 89* (1-4), pp-1067-1079.
[12] FRENCH, A. N., JACOB, F., ANDERSON, M. C., KUSTAS, W. P., TIMMERMANS, W., GIESKE, A., SU, B., SU, H., MCCABE, M. F., LI, F., PRUEGER, J. H. AND BRUSNELL, N., 2005: Surface energy fluxes with the Advanced Spaceborne Thermal Emission and Reflection radiometer (ASTER) at the Iowa 2002 SMACEX site (USA). *Rem. Sens. Environ. 99* (1-2), pp. 55-65.
[13] JACOB, F, PETITCOLIN, F.; SCHMUGGE, T.; VERMOTE, E.; FRENCH, A.; OGAWA, K. 2004: Comparison of land surface emissivity and radiometric temperature derived from MODIS and ASTER sensors. *Rem. Sens. Environ. 90(2)*, pp. 137-152.
[14] LÓPEZ-BERMÚDEZ, F., BOIX-FAYOS, C., SOLÉ-BENET, A., ALBALADEJO, J., BARBERÁ, G.C., DELBARRIO,G., CASTILLO, V., GARCÍA, J., LÁZARO, R., MARTÍNEZ-MENA, M.D., MOSCH, W., NAVARRO-CANO, J.A., PUIGDEFÁBREGAS, J., SANJUÁN,M. 2005: Landscapes and desertification in south-east Spain; overview and field sites. Field Trip Guide A-5. *6th International Conference on Geomorphology. Sociedad Española de Geomorfología*. 40 pp.
[15] LIANG S., 2000: Narrowband to broadband conversions of land surface albedo I Algorithms. *Rem. Sens. Environ. 76*, pp. 213-238.
[16] FU, P. AND RICH M. 2002: A geometric solar radiation model with applications in agriculture and forestry. *Comput. Electron. Agr*. 37 (2002): 25-35.
[17] VAN DE GRIEND A.A AND OWE M, 1993: On the relationship between thermal emissivity and the normalized difference vegetation index for natural surfaces, *Int. J. Remote Sens. 14(6)*, pp. 1119-1131.
[18] IDSO, S.B., JACKSON, R.D. 1969: Thermal radiation from the atmosphere. *J. Geophys.Res. 74*, pp. 5397–5403.
[19] CZAJKOWSKI, K.P., S.N.GOWARD, T. MULHERN, S.J. GOETZ, A. WALZ, D.SHIREY, S. STADLER, S.D.PRINCE, AND DUBAYAH, R.O., 2000: Estimating environmental variables using thermal remote sensing. In: D. A. Quattrochi and Jeffrey C. Luvall (eds.): *Thermal remote sensing in land surface processes*. CRC Press. Pp. 11-32.
[20] ROERINK, G. J., SU, Z. AND M. MENENTI. 2000: S-SEBI: A Simple Remote Sensing Algorithm to Estimate the Surface Energy Balance. *Phys. Chem. Earth 25*, pp. 147-157.
[21] BASTIAANSSEN, W.G.M., MENENTI, M., FEDDES, R.A., HOLTSLAG, A.A.M., 1998: A remote sensing surface energy balance algorithm for land (SEBAL) 1. Formulation. *J. Hydrol. 212-213* (1-4) pp. 198-212.
[22] DEL BARRIO G., M. SANJUAN, J. PUIGDEFABREGAS, M. BOER AND STELLMES, M., 2005: Assessing land condition through a bi-dimensional index of vegetation Rainfall Use Efficiency: the case of mainland Spain. Remote Sensing and Geoinformation Processing in the Assessment and Monitoring of Land Degradation and Desertification. Trier, September 2005. Abstract book. Pp. 87-88.
[23] HARGREAVES, G. H. AND Z. A. SAMANI. 1982: Estimating potential evapotranspiration. *J. Irrig. Drain E-ASCE.* 108: 225-230.
[24] BALDOCCHI, D. D., FALGE, E., GU, L., OLSON, R., HOLLINGER, D., RUNNING, S., ANTHONI, P., BERNHOFER, CH., DAVIS, K., FUENTES, J., GOLDSTEIN, A., KATUL, G., LAW, B., LEE, X., MALHI, Y., MEYERS, T., MUNGER, J. W., OECHEL, W., PILEGAARD, K., SCHMID, H. P., VALENTINI, R., VERMA, S., VESALA, T., WILSON K. & WOFSY, S., 2001: FLUXNET: A new tool to study the temporal and spatial variability of ecosystem-scale carbon dioxide, water vapor and energy flux densities. *B. Am. Meteorol. Soc. 82*, pp. 2415 - 2434.
[25] WERE, A., 2005: Agregación espacial de la evapotranspiración en clima semiárido. *Ph.D. Thesis* (in Spanish). Universidad de Almeria, Spain. Pp.212
[26] SEGUIN, B., BECKER, F., PHULPIN, T., GU, X.F., GUYOT, G., KERR, Y., KING, C., LAGOUARDE, J.P., OTTLE, C., STOLL, M:P:, TABBAGH, A., AND VIDAL, A. 1999: IRSUTE: A Minisatellite Project for Land Surface Heat Flux Estimation form Field to Regional Scale. *Rem. Sens. Environ. 68*, pp. 357-369.
[27] HUMES, K., HARDY, R., KUSTAS, W., PRUEGER, J. AND STARKS, P., 2000: High spatial resolution mapping of surface energy balance components with remotely sensed data. In: D. A. Quattrochi and Jeffrey C. Luvall (eds.): *Thermal remote sensing in land surface processes.* CRC Press. Pp. 110-132.
[28] LAYMON, C, A. AND QUATTROCHI, D.A.., 2000: Estimating spatially-distributed surface fluxes in a semi-arid Great Basin desert using Landsat TM thermal data. In: D. A. Quattrochi and Jeffrey C. Luvall (eds.): *Thermal remote sensing in land surface processes*. CRC Press. Pp. 110-132.